JUSTC

Article

http://justc.ustc.edu.cn

Received: February 23, 2022; Accepted: April 01, 2022

Unruh effect of multiparticle states and black hole radiation

Jianyu Wang[1,2,3] ✉

[1]*Department of Astronomy, School of Physical Sciences, University of Science and Technology of China, Hefei 230026, China;*
[2]*CAS Key Laboratory for Researches in Galaxies and Cosmology, University of Science and Technology of China, Hefei 230026, China;*
[3]*School of Astronomy and Space Science, University of Science and Technology of China, Hefei 230026, China*

✉Correspondence: Jianyu Wang, E-mail: emc@mail.ustc.edu.cn

Graphical abstract

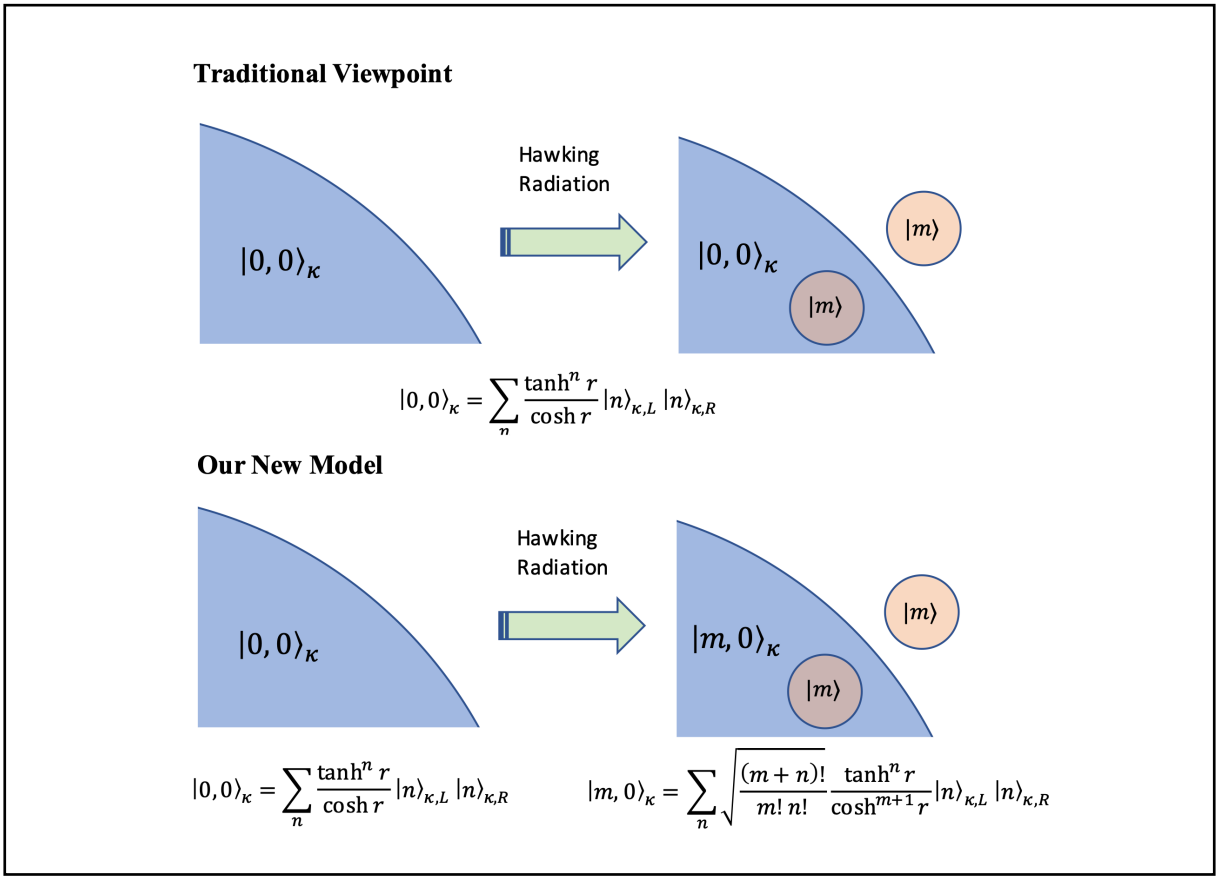

The state of the black hole horizon will shift after particle radiated in our toy model. Such a black hole will have the memory effect and the entropy of radiation can reproduce the Page curve. At the same time this horizon shift cannot be measured locally.

Public summary

- Unruh effect of multiparticle is studied in both left and right wedge of Rindler spacetime.
- A toy model of quantum black hole is constructed. The state of black hole horizon will evolve when particles fall in or emit out.
- This black hole radiation model reproduces the Page curve.

Citation: Wang J Y. Unruh effect of multiparticle states and black hole radiation. *JUSTC*, **2022**, 52(6): 4. DOI: 10.52396/JUSTC-2022-0039

JUSTC

Article

http://justc.ustc.edu.cn

Received: February 23, 2022; Accepted: April 01, 2022

Unruh effect of multiparticle states and black hole radiation

Jianyu Wang[1,2,3] ✉

[1]Department of Astronomy, School of Physical Sciences, University of Science and Technology of China, Hefei 230026, China;
[2]CAS Key Laboratory for Researches in Galaxies and Cosmology, University of Science and Technology of China, Hefei 230026, China;
[3]School of Astronomy and Space Science, University of Science and Technology of China, Hefei 230026, China

✉Correspondence: Jianyu Wang, E-mail: emc@mail.ustc.edu.cn

Cite This: *JUSTC*, **2022**, 52(6): 4 (8pp) Read Online

Abstract: In this study, we investigated the field under the Unruh effect. The energy and entanglement properties of the single-mode q-particle states were discussed. We found that in the non-inertial reference frame $|q,0\rangle_\alpha$ states exhibit a similar energy spectrum to vacuum $|0,0\rangle_\alpha$, but with different entanglement properties. With respect to an application, we proposed a black hole radiation model, assuming that states near the horizon are constructed via q-particle states. We calculated the evolution of the entanglement entropy of radiation and proved that our model can reproduce the Page curve. Hence, this can be considered as an indication solution of the black hole information paradox.

Keywords: black hole; Unruh effect; quantum information

CLC number: P14; O41 **Document code:** A

1 Introduction

According to the Unruh effect[1–6], quantum fields in Minkowski spacetime will have thermal properties when observed by a uniformly accelerated observer. For example, in the accelerating reference frame, the ground state of an inertial observer is considered as a mixed state in thermodynamic equilibrium at a temperature of $T=\alpha/(2\pi)$. The Unruh effect plays an essential role in understanding motion in the presence of a horizon and, most importantly, in understanding Hawking radiation[7–13]. In this study, we discuss the Unruh effect of the single-mode states $|0,q\rangle_\alpha$ and $|q,0\rangle_\alpha$. There are q-excited states in a non-inertial frame with acceleration α. The $|q,0\rangle_\alpha$ states represent particles excited in the left Rindler wedge, which is unreachable for a right Rindler wedge observer. However, we determined that these excited particles affect the right-wedge spacetime via entanglement. We propose a black hole radiation model based on the assumption that the black hole horizon is formed by the $\{|q,0\rangle\}$ states. The black hole radiation in our model will not always be a maximally mixed state, but the entanglement will change over time. Furthermore, the entropy of radiation is consistent with the Page curve. Thus, this model can preserve the quantum unitarity in the black hole radiation process and this type of information paradox does not appear.

The remainder of this paper is organized as follows. In Section 2, Unruh effect and Hawking radiation are reviewed. Unruh effect occurs when detecting fields in a non-inertial frame, where observed fields will be in mixed thermal states and particles will be emitted. In Section 3, we discuss the q-excited states $|0,q\rangle_\alpha$ and $|q,0\rangle_\alpha$. In particular, we examine the energy and entanglement properties. When measuring their energy, the $|q,0\rangle_\alpha$ states function similar to $(q+1)$ copies of vacuum states. Nevertheless, their entanglement is the same as $|0,q\rangle_\alpha$. Unruh effect occurs near black hole horizons, when the surface gravity κ plays the role of proper acceleration α, and the black hole event horizon divides spacetime into unreachable wedges. Particle pairs are created near the horizon, and Hawking radiation occurs. In Section 4, we propose a black hole radiation model using Unruh effect theory. Our model maintains the horizon energy spectrum of the traditional black hole model, but the entanglement between radiation and the black hole changes after the particles fall in the black hole. This allows the black hole horizon to exhibit a memory effect. We calculate the evolution of radiation entropy during the Hawking radiation process. Furthermore, the results show that our model could reproduce the Page curve. Such these entangled two-wedge states can be considered as an indication of a solution to the information paradox.

2 Unruh effect

This section briefly reviews the Unruh effect of a scalar field. Fermion fields were examined in Refs. [14–17] and were reported to exhibit a similar Unruh effect. A massless real scalar quantum field $\phi(x,t)$ obeys the Klein-Gordon equation $g^{\mu\nu}\partial_\mu\partial_\nu\phi=0$. In the Minkowski metric:

$$\mathrm{d}s^2=-\mathrm{d}t^2+\mathrm{d}x^2+\mathrm{d}y^2+\mathrm{d}z^2 \tag{1}$$

a free scalar field can be formally solved as:

$$\phi=\sum_k(\hat{a}_k^\dagger u_k^*+\hat{a}_k u_k) \tag{2}$$

where $\{u^*,u\}$ is a complete set of Klein-Gordon solutions of the free scalar field in Minkowski spacetime. $\hat{a}_k^\dagger$ and $a_k^\dagger$ are creation and annihilation operators for k-mode. The vacuum state $|0\rangle$ is defined as follows:

DOI: 10.52396/JUSTC-2022-0039
JUSTC, **2022**, 52(6): 4

$$a_k|0(k)\rangle = 0 \tag{3}$$

and n-particle states are defined as follows:

$$\frac{1}{\sqrt{n!}}(a^\dagger)^n|0(k)\rangle = |n(k)\rangle \tag{4}$$

These $\{|n(k)\rangle\}$ states constitute a Fock space of the k-mode.

Fields living in a non-inertial frame have been widely discussed[18–21]. If the constant proper acceleration α is along "x" direction, the new reference frame (η, ξ, y, z) is Rindler space (shown in Fig. 1).

Rindler space divides the entire spacetime into four wedges, and at least two wedges are required to construct a Cauchy surface. For instance, we considered fields in the left and right wedges. With respect to the right wedge ($x > 0$ and $|x| < |t|$), the transformation between Rindler coordinate and Minkowski coordinates is as follows:

$$t = \alpha^{-1}\mathrm{e}^{\alpha\xi}\sinh\alpha\eta \tag{5}$$

$$x = \alpha^{-1}\mathrm{e}^{\alpha\xi}\cosh\alpha\eta \tag{6}$$

and for left wedge ($x < 0$ and $|x| < |t|$), the transformation is:

$$t = -\alpha^{-1}\mathrm{e}^{\alpha\xi}\sinh\alpha\eta \tag{7}$$

$$x = -\alpha^{-1}\mathrm{e}^{\alpha\xi}\cosh\alpha\eta \tag{8}$$

With the transformation formula above, the metric for Rindler space is:

$$\mathrm{d}s^2 = \mathrm{e}^{2\alpha\xi}(-\mathrm{d}\eta^2 + \mathrm{d}\xi^2) + \mathrm{d}y^2 + \mathrm{d}z^2 \tag{9}$$

The Klein-Golden equation can be solved for the left and right wedges, and thus we obtain two sets of solutions: $\{h(x,t)_{k,L}, h(x,t)^*_{k,L}\}$ for the left wedge and $\{h(x,t)_{k,R}, h(x,t)^*_{k,R}\}$ for the right wedge. These two sets together construct a complete basis for a scalar field in Rindler space. Typically, a free scalar field can be expanded in Rindler space as follows:

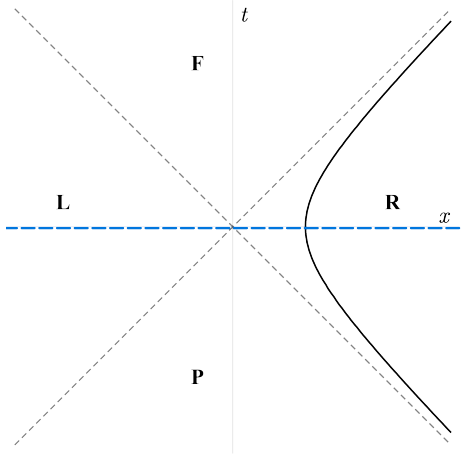

Fig. 1. Rindler space. Spacetime is divided into four wedges, left "L", right "R", future "F", and past "P". The black full line represents the trajectory with constant acceleration. The blue long dashed line is an example of the Cauchy surface. Both the left and right wedges are required to cover the entire space.

$$\phi = \sum_k \left(\hat{a}_{k,L}h_{k,L} + \hat{a}^\dagger_{k,L}h^*_{k,L} + \hat{a}_{k,R}h_{k,R} + \hat{a}^\dagger_{k,R}h^*_{k,R}\right) \tag{10}$$

where $\{\hat{a}_{k,L}, \hat{a}^\dagger_{k,L}\}$ and $\{\hat{a}_{k,R}, \hat{a}^\dagger_{k,R}\}$ are the k-mode annihilation and creation operators in the left and right wedges of Rindler space. Furthermore, a Fock space, $\{|n_1\rangle_L|n_2\rangle_R\}$, can be generated by these operators.

For an accelerated observer, the Rindler horizon is located at $1/\alpha$ in the direction opposite to the acceleration[22]. When the acceleration is significant, only a small region can be detected in the direction opposite to the acceleration. By contrast, the right wedge can cover a vast space in the opposite direction when the acceleration is infinitesimal. In this study, we also divide the entire Minkowski spacetime into four patches by considering the limit $\alpha \to 0$ of Rindler space. In the $\alpha \to 0$ limit, the Rindler horizon is located infinitely far from the observer and the right wedge covers an infinitely large spacetime around the observer. Under this notion, the Hilbert space of quantum fields in Minkowski spacetime can be formally expressed as follows:

$$H_M = H_{0,L} \otimes H_{0,R} \tag{11}$$

An observer is living in the R region, and L region can be considered as the boundary effect. A Minkowski vacuum state has the form $|0\rangle_M = |0\rangle_{0,L}|0\rangle_{0,R}$. Additionally, the operator should be expressed as $O_M = \mathbb{1}_L \times O_R$. For example, the annihilation operator $\hat{a}_{M,k}$ has the form $\hat{a}_{M,k} = \mathbb{1}_{L,k} \times \hat{a}_{R,k}$.

Here, we observe that the same field is expanded in Minkowski spacetime (Eq. (2)) and Rindler space (Eq. (10)). These two expressions are equal, which indicates the relation between the expression of fields in these different frames:

$$|\psi\rangle_\alpha = \boldsymbol{U}(\alpha)|\psi\rangle_0, \tag{12}$$

where $|\psi\rangle_\alpha$ denotes the field state ψ observed in non-inertial frame with proper acceleration α, and $|\psi\rangle_0$ denotes the field state observed in Minkowski spacetime. Here, $\boldsymbol{U}(\alpha)$ denotes the Bogoliubov transformation, which is a unitary operator that can be expressed as follows:

$$\boldsymbol{U}(\alpha) = \mathrm{e}^{-r(\alpha)(\hat{a}_L\hat{a}_R - \hat{a}^\dagger_L\hat{a}^\dagger_R)} \tag{13}$$

where $r(\alpha)$ denotes an acceleration-related parameter defined by $\tanh r(\alpha) = \mathrm{e}^{-\pi\omega/\alpha}$.

For instance, the single-mode Minkowski vacuum $|0\rangle_M \equiv |0,0\rangle_0$ is an entangled state in Rindler space[15, 23, 24]:

$$\begin{aligned}|0,0\rangle_\alpha =& \boldsymbol{U}(\alpha)|0,0\rangle_0 = \\ & \frac{1}{\cosh r}\exp(\tanh r\hat{a}^\dagger_L\hat{a}^\dagger_R)|0\rangle_L|0\rangle_R = \\ & \frac{1}{\cosh r}\sum_n \tanh^n r|n\rangle_L|n\rangle_R\end{aligned} \tag{14}$$

The accelerated observer can only detect a field in one of the wedges, such that only a part of the field can be detected. For example, the number operator for a right-wedge Rindler observer is $N_R = \mathbb{1}_L \times \hat{a}^\dagger_R\hat{a}_R$. Operating on the state above, the expected particle number of a Minkowski vacuum is as follows:

$$\langle 0,0|N|0,0\rangle_\alpha = \sinh^2 r = \frac{1}{\mathrm{e}^{2\pi\omega/\alpha} - 1} \tag{15}$$

DOI: 10.52396/JUSTC-2022-0039
JUSTC, **2022**, 52(6): 4

A Minkowski vacuum $|0,0\rangle_0$ is not a ground state in a non-inertial frame. Conversely, a Rindler vacuum is also an excited state in the inertial frame. This corresponds to the Unruh effect. Moreover, Eq. (15) agrees with the Bose-Einstein distribution at temperature $T=\alpha/(2\pi)$. Consequently, a Minkowski vacuum corresponds to a hot bath in an accelerated frame, and particle radiation occurs in the black-body spectrum.

3 Unruh effect of q-particle states

A q-particle Minkowski state in Hilbert space (Eq. (11)) can be formally described as follows:

$$|q\rangle_M = |0,q\rangle_0 \tag{16}$$

When q-excitation wave is sharp and located near the accelerated observer, the pulse assumption can be used safely. In any accelerating frame, the excited particles are located in the right wedge of Rindler space. These q-excited wave pulses can be evaluated using the Bogoliubov transformation as follows:

$$\begin{aligned}|0,q\rangle_\alpha =&\mathrm{e}^{-r(\hat{a}_L\hat{a}_R-\hat{a}_L^\dagger\hat{a}_R^\dagger)}|0,q\rangle_0 = \\ &\exp[\tanh r\,\hat{a}_L^\dagger\hat{a}_R^\dagger]\exp[-\ln\cosh r(\hat{a}_L\hat{a}_L^\dagger+\hat{a}_R^\dagger\hat{a}_R)]\cdot \\ &\exp[-\tanh r\,\hat{a}_L\hat{a}_R]0\rangle_L|q\rangle_R = \\ &\frac{1}{\cosh^{q+1} r}\sum_n \tanh^n r\sqrt{\frac{(q+n)!}{q!n!}}|n\rangle_L|n+q\rangle_R = \\ &\sum_n f_n(q,\tanh r)|n\rangle_L|n+q\rangle_R\end{aligned} \tag{17}$$

Here, the coefficient function $f_n(q,\tanh r)$ is defined as follows:

$$f_n(q,\tanh r) = \sqrt{(q+n)!/(q!n!)}\tanh^n r/\cosh^{q+1} r \tag{18}$$

By tracing the left wedge, the density matrix for the right wedge is as follows:

$$\rho_{R,0q} = \sum_n f_n^2(q,\tanh r)|n+q\rangle_R\langle n+q| \tag{19}$$

In previous studies, the form $|0,q\rangle$ was used to indicate the Minkowski q-particle states observed in a non-inertial frame. It can be considered the case that the pulse was near the accelerated observer. However, in general, when transforming a Minkowski creation operator $a_0^\dagger$ to Rindler space, we can state the following relation[25]:

$$\hat{a}_\alpha^\dagger = \boldsymbol{U}^\dagger(\alpha)(\gamma_L\hat{a}_{L,0}^\dagger\times\mathbb{1}_R+\gamma_R\mathbb{1}_L\times\hat{a}_{R,0}^\dagger)\boldsymbol{U}(\alpha) \tag{20}$$

where $|\gamma_L|^2+|\gamma_R|^2=1$. In states $|0,q\rangle_\alpha$, parameters $\gamma_L=0$ and $\gamma_R=1$ are selected. In the following, we select another extreme case: the excitations are infinitely far from the observer and in the opposite orientation of acceleration. In such a situation, these excitations are all located at the left wedge, and parameters $\gamma_L=1$ and $\gamma_R=0$ should be chosen, i.e.,

$$\hat{a}_\alpha^\dagger = \boldsymbol{U}^\dagger(\alpha)(\hat{a}_{L,0}^\dagger\times\mathbb{1}_R)\boldsymbol{U}(\alpha) \tag{21}$$

We formally describe these excited q-particle states as $|q,0\rangle_\alpha$ for Rindler space and $|q,0\rangle_0$ for Minkowski spacetime, indicating that these excitations are always behind the Rindler horizon for any acceleration α. Rindler state $|q,0\rangle_\alpha$ can also be generated by Bogoliubov transformation from Minkowski state $|q,0\rangle_0$:

$$\begin{aligned}|q,0\rangle_\alpha =&\boldsymbol{U}(\alpha)|q,0\rangle_0 = \\ &\frac{1}{\cosh^{q+1} r}\sum_n\sqrt{\frac{(q+n)!}{q!n!}}\tanh^n r|n+q\rangle_L|n\rangle_R = \\ &\sum_n f_n(q,\tanh r)|n+q\rangle_L|n\rangle_R\end{aligned} \tag{22}$$

For a right-wedge observer, the density matrix is as follows:

$$\boldsymbol{\rho}_{R,q0} = \sum_n f_n^2(q,\tanh r)|n\rangle_R\langle n| \tag{23}$$

These formulas exhibit the same coefficient values with $|0,q\rangle_\alpha$ but different bases.

As expected, when considering the limit $\alpha\to 0$ ($\tanh r\to 1$), the expressions of $|0,q\rangle_\alpha$ and $|q,0\rangle_\alpha$ will decay to Minkowski $|0,q\rangle_0$ and $|q,0\rangle_0$. Moreover, under the limit $\alpha\to 0$, the right wedge density matrices $\boldsymbol{\rho}_{R,0q}$ and $\boldsymbol{\rho}_{R,q0}$ will decay to $|q\rangle\langle q|$ and $|0\rangle\langle 0|$. Therefore, we consider that the forms of $|q,0\rangle_\alpha$ and $|q,0\rangle_0$ are valid for discussing field states in a non-inertial frame under the assumption.

We plotted the coefficient $f_n(q,\tanh r)$ with different q values (fixing the acceleration parameter $\tanh r$) in Fig. 2 and with different $\tanh r$ values (fixing q) in Fig. 3. The figures show that the coefficient has one peak, and when $q=0$, the peak is always at $n=0$. For $q\neq 0$, the peak occurs at $n=\cosh^2 r((q+1)\tanh^2 r-1)$. As the values of q and α increase, the peak moves to the right.

3.1 Energy distribution

Acting as the right wedge number operator on the q-excited states $|q,0\rangle_\alpha$ and $|0,q\rangle_\alpha$, we obtain the expectation value of the right wedge particle number:

$$n_{q0} = \langle q,0|N|q,0\rangle_\alpha = (q+1)\sinh^2 r \tag{24}$$

$$\begin{aligned}n_{0q} = \langle 0,q|N|0,q\rangle_\alpha =&q\cosh^2 r+\sinh^2 r = \\ &q+(q+1)\sinh^2 r\end{aligned} \tag{25}$$

In the zero-acceleration limit ($\tanh r\to 0$), n_{0q} approaches q and n_{q0} approaches 0. This result is consistent with $|0,q\rangle_0$ and $|q,0\rangle_0$, the q-particle state in Minkowski spacetime.

Moreover, as Minkowski vacuum agrees with the single-particle Bose-Einstein distribution, n_{q0} obeys the $(q+1)$-particles Bose-Einstein distribution, with $(q+1)$ times the particle number of the vacuum $|0,0\rangle$:

$$n_{q0} = \frac{(q+1)}{\mathrm{e}^{2\pi\omega/\alpha}-1} \tag{26}$$

Additionally, n_{q0} functions as q excited particles in a $(q+1)$ thermal vacuum:

$$n_{0q} = q+\frac{(q+1)}{\mathrm{e}^{2\pi\omega/\alpha}-1} \tag{27}$$

If we place a particle detector in the right wedge of $|q,0\rangle_\alpha$, then, on average, we will obtain the same particle number as

DOI: 10.52396/JUSTC-2022-0039
JUSTC, 2022, 52(6): 4

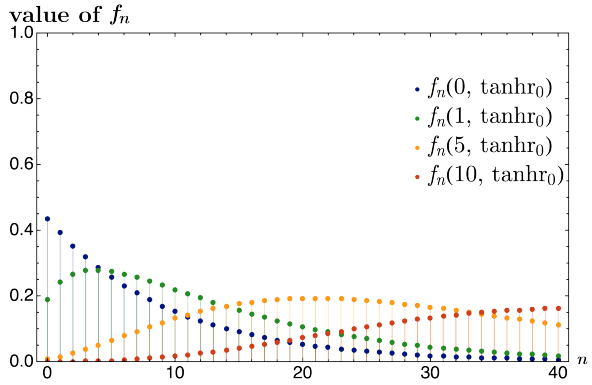

Fig. 2. Coefficient function $f_n(q,\tanh r)$ for different q. The horizontal axis represents n, and the vertical axis represents the value of $f_n(q,\tanh r)$. The figures show that as q increases, the peak of $f_n(q,\tanh r)$ moves to the right, and the distribution becomes more "even".

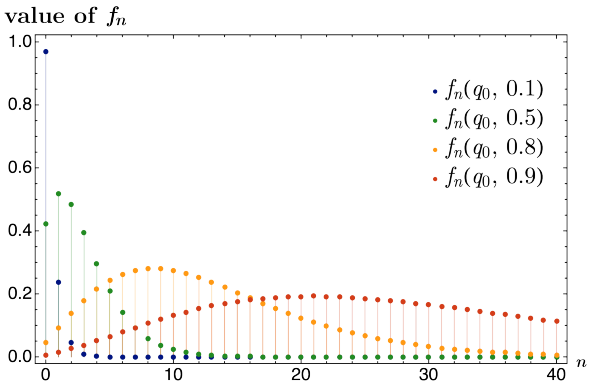

Fig. 3. Coefficient function $f_n(q,\tanh r)$ for different $\tanh r$ (different acceleration). The horizontal axis represents n, and the vertical axis represents the value of $f_n(q,\tanh r)$. The figures show that as $\tanh r$ (larger acceleration) increases, the peak of $f_n(q,\tanh r)$ moves to the right, and the distribution becomes more "even".

the state $|0,0\rangle_\alpha|0,0\rangle_\alpha\cdots|0,0\rangle_\alpha$, which is a system with $(q+1)$ vacua.

3.2 Entanglement between left and right wedges

In this section, we discuss entanglement properties. The entanglement in the Unruh effect has exciting features[26–29]. An entangled state is defined as a state that cannot be factored as the product state of the subsystems. They are not individual particles but an inseparable state. One measurement of quantum entanglement corresponds to von Neumann entropy, which is defined as follows:

$$S = -\mathrm{Tr}\boldsymbol{\rho}\ln\boldsymbol{\rho} \tag{28}$$

It is a useful tool to quantify the entanglement of pure states. Suppose a pure state is formed by subsystems A and B. The von Neumann entropy of subsystem A quantifies the quantum entanglement between A and B. And if $S_A = 0$, A and B are not entangled.

For Rindler states $|q,0\rangle_\alpha$ and $|0,q\rangle_\alpha$, we can calculate the right-wedge von Neumann entropy to quantify the entanglement between the left and right wedges.

First, consider the case of $q = 0$ and the vacuum states. The right-wedge density matrix of Minkowski vacuum state $|0,0\rangle_\alpha$ is:

$$\boldsymbol{\rho}_R = \mathrm{Tr}_L\boldsymbol{\rho}_{LR} = \frac{1}{\cosh^2 r}\sum_n \tanh^{2n} r|n\rangle_R\langle n| \tag{29}$$

The von Neumann entropy is as follows:

$$\begin{aligned} S_R &= -\mathrm{Tr}\boldsymbol{\rho}_R\ln\boldsymbol{\rho}_R = \\ &-\sum_n\left[\frac{1}{\cosh^2 r}\tanh^{2n} r\right] = \\ &-2\sinh^2 r\ln\tanh^2 r - \ln\cosh^2 r \end{aligned} \tag{30}$$

This is a generally a non-zero value. Therefore, the Minkowski vacuum state is entangled state in the accelerating reference frame. In the limit $\alpha\to 0$, entropy $S_R\to 0$ returns to the result of Minkowski vacuum that the right wedge is in a pure state. For the limit $\alpha\to\infty$, entropy $S_R\to\infty$.

Then, we discuss $q\neq 0$, the q-excited states $|0,q\rangle_\alpha$, and $|q,0\rangle_\alpha$. The right wedge reduces the density matrix $\boldsymbol{\rho}_R$ of $|q,0\rangle_\alpha$ as follows:

$$\boldsymbol{\rho}_R = \frac{1}{\cosh^{2q+2} r}\sum_n \frac{(q+n)!}{q!n!}\tanh^n r|n\rangle_R\langle n| \tag{31}$$

The von Neumann entropy is as follows:

$$\begin{aligned} S_R = \sum_n \frac{(q+n)!}{q!n!}\frac{1}{\cosh^{2q+2} r}\tanh^{2n} r\cdot \\ \ln\left(\frac{(q+n)!}{q!n!}\frac{1}{\cosh^{2q+2} r}\tanh^{2n} r\right) \end{aligned} \tag{32}$$

With the same q_0, the right wedge density matrices of $|0,q_0\rangle_\alpha$ and $|q_0,0\rangle_\alpha$ exhibit the same eigenvalues, and the entropy is equal.

By considering Eq. (32) to the limit $\alpha\to 0$, the entropy goes to zero ($S_R\to 0$), and the limit $\alpha\to\infty$, the entropy goes to infinity ($S_R\to\infty$). We plot the subsystem entropy of different $|q,0\rangle_\alpha$ states in Fig. 4. We directly observe that the $|q,0\rangle_\alpha$ state exhibits a larger entropy than $|0,0\rangle_\alpha$. However, they simultaneously have $(q+1)$ times the expected particle number (energy). As previously shown, the energy of the right wedge $|q,0\rangle_\alpha$ functions in a $(q+1)$ vacuum state. We normalized the entanglement $\tilde{S} = S/(q+1)$ to compare the entanglement with the same energy. Furthermore, We numerically plotted the normalized entropy of $|q,0\rangle_\alpha$(shown in Fig. 5). Although the entropy increases as q increases, and the normalized entropy decreases and vacuum state $|0,0\rangle_\alpha$ exhibits the largest value. In Refs. [30] and [31], it has been proved that $|0,0\rangle_\alpha$ is a maximally entangled state, which is consistent with our results.

4 Application of left wedge excited states

First, we review and conclude the previous discussion on the $|q,0\rangle_\alpha$ states. To make this form valid for any acceleration α, we limit these q excitations to those located at the infinity of Minkowski spacetime, such as when translating to Rindler space. These excitations are behind the horizon and located in the left wedge. Under these assumptions, $|q,0\rangle_\alpha$ states have the following properties:

(i) Energy spectrum. For a non-inertial observer ($\alpha=\kappa$), as shown before, the energy spectrum of the $|q,0\rangle_\alpha$ state is $(q+1)\omega\sinh^2 r$, which is same to $(q+1)$ times the vacuum

DOI: 10.52396/JUSTC-2022-0039
JUSTC, 2022, 52(6): 4

states $|0,0\rangle_\alpha$. This is the energy distribution for $(q+1)$ Bose-Einstein particles at temperature $T=\alpha/(2\pi)$. For an inertial observer ($\alpha=0$), the particles are at infinity far, so particle will be observed.

(ii) Excitation particles. For a non-inertial observer ($\alpha=\kappa$), the peak of coefficient function $f_n(q,\tanh r)$ (shown in Fig. 2 and Fig. 3) moves to a larger n when the value of q and acceleration α increases. This indicates that when $q\neq 0$, a larger q and α are more likely to radiate highly excited particles. However, when $q=0$, the peak of the vacuum state is always at $n=0$. For an inertial observer ($\alpha=0$), the only non-zero value of coefficient function is when $n=0$ and $f_0(q,0)\equiv 1$, which implies that the fields are in vacuum states and no particle is emitted.

(iii) Entanglement. For a non-inertial observer ($\alpha=\kappa$), although with the same energy, $|q,0\rangle_\alpha$ states exhibit less entanglement between the left and right wedges than $(q+1)$ vacuum states. As q in $|q,0\rangle_\alpha$ state increases, the entanglement between the two wedges decreases. For an inertial observer ($\alpha=0$), the entanglement between the q particles is zero.

Although at classical level, these left-wedge-excited particles are unreachable by a right-wedge observer, they can affect the right wedge via quantum entanglement. Different from $|0,0\rangle_\alpha$, $|q,0\rangle_\alpha$ states lead the horizon to emit more excited particles. Simultaneously, these $|q,0\rangle_\alpha$ states exhibit the same energy distribution as $|0,0\rangle_\alpha$.

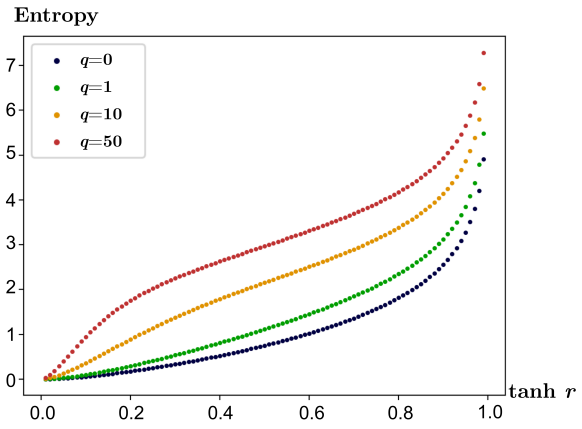

Fig. 4. Right wedge von Neumann entropy for different $|q,0\rangle_\alpha$ states along with $\tanh r$. Four curves from bottom to top are $q=0,1,10,50$. Entropy increases as acceleration increases. Simultaneously, a larger q leads to larger entropy.

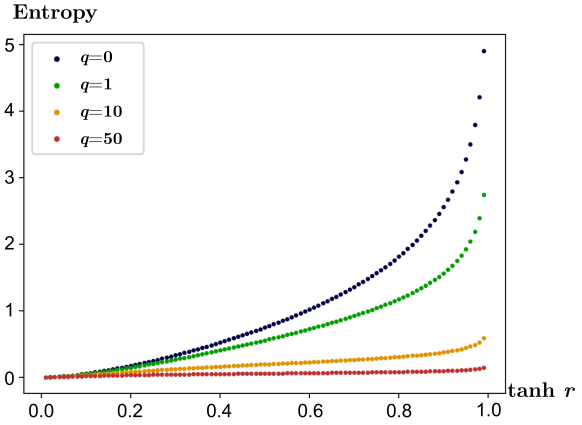

Fig. 5. "Normalized entropy" along with $\tanh r$ to compare right wedge entropy of different q when fixing the energy. Four curves from bottom to top are $q=50$, 10, 1, 0. This shows that vacuum $q=0$ leads to the largest entropy, and a larger q leads to less "normalized entropy".

One important application of the Unruh effect is in fields near the black hole horizon[32–35]. The black hole surface gravity κ plays the role of proper acceleration α. According to the Einstein equivalency principle, the black hole horizon is a vacuum for a free-falling observer. However, for an infinity observer, the black hole horizon is in the state:

$$|0,0\rangle_\kappa=\sum_n\frac{\tanh^n r}{\cosh r}|n\rangle_{\kappa,L}|n\rangle_{\kappa,R} \tag{33}$$

By tracing the unreachable left-wedge region, we obtain:

$$\boldsymbol{\rho}_R=\sum_n^\infty\frac{\tanh^{2n} r}{\cosh^2 r}|n\rangle_R\langle n| \tag{34}$$

which is the horizon state observed by an infinity observer. Therefore, the black hole emits particles in black-body radiation in temperature $T=\kappa/(2\pi)$. Moreover, this state indicates that when $|n\rangle_R$ particles are emitted, $|n\rangle_L$ particles fall into the horizon. Given that the radiation particles are maximally entangled with the infalling particles. The radiation is in a maximally mixed state.

Hence, an information paradox[36–38] of black hole radiation occurs as follows: black body radiation does not carry any information except temperature; therefore, when the black hole finally evaporates, all the information of particles falling into the black hole will lose. And from the infalling matter to radiation particles, quantum state evaluates from a pure state to a mixed state. This violates the basic quantum mechanical principle that the physical processes should be unitary.

We propose a black hole radiation model based on these $|q,0\rangle$ states. At the beginning, the black hole horizon state is $|0,0\rangle_\kappa$. Then, particle pairs are created. The right-wedge particles radiate to infinity, and the left-wedge particles will fall into black hole singularity, and shift the horizon state. Such that the whole state of horizon and radiation transforms to:

$$\sum_n\frac{\tanh^n r}{\cosh r}|n,0\rangle_\kappa|n\rangle \tag{35}$$

If the radiation is measured, then it exhibits a probability of $\tanh^{2q} r/\cosh^2 r$ to observe q-emitted particles. After the measurement, the black hole horizon is in state $|q,0\rangle_\kappa$, and the radiation process continues as follows:

$$\begin{aligned}|q,0\rangle_\kappa=&\frac{1}{\cosh^{q+1} r}\sum_n\sqrt{\frac{(q+n)!}{q!n!}}\tanh^n r|n+q,n\rangle_\kappa\rightarrow\\&\frac{1}{\cosh^{q+1} r}\sum_n\sqrt{\frac{(q+n)!}{q!n!}}\tanh^n r|n+q,0\rangle_\kappa|n\rangle\end{aligned} \tag{36}$$

After m steps, the entire state changes to:

DOI: 10.52396/JUSTC-2022-0039
JUSTC, **2022**, 52(6): 4

$$|0,0\rangle_\kappa \to \sum_{n_m=0}\sum_{n_{m-1}=0}^{n_m}\cdots\sum_{n_1=0}^{n_2} f_{n_m-n_{m-1}}(n_{m-1},\tanh r_m)\cdots f_{n_1}(0,\tanh r_1)|n_m,0\rangle_{\kappa_m}|n_m-n_{m-1}\rangle\cdots|n_1\rangle \quad (37)$$

Here, the surface gravity κ (and r) changes over time based on the current black hole mass, i.e. $\tanh r_0 < \tanh r_1 < \cdots < \tanh r_{m-1}$. Therefore, the radiation process has a memory effect and can preserve the information.

Next, we show that this model can reproduce the Page curve that describes the "average" entropy of a bipartite system[39, 40]. We consider that the entire system is in a pure quantum state $|\psi\rangle_{AB}$. The Hilbert space dimension of subsystem A is m, and the dimension of subsystem B is n. The calculation of Page tells us that the "average" entropy of subsystem A (or B. For a pure state $|\psi\rangle_{AB}$, $S_A = S_B$) is (when $m \leqslant n$):

$$S_a = \sum_{k=n+1}^{mn}\frac{1}{k} - \frac{m-1}{2n} \quad (38)$$

It can be concluded from this formula that these two subsystems are nearly maximally entangled when $m \ll n$. The entropy of subsystem A increases before Page time (when $m < n$) and decreases after Page time (when $m > n$). With respect to black-hole radiation, the entropy of radiation increases at an early time and decreases at the later time. The just radiated particles are maximally entangled with the black hole at the beginning, and the entanglement decreases during the radiation process.

In our radiation model, after q particles are emitted, the black hole horizon shifts from $|0,0\rangle_\kappa$ to $|q,0\rangle_\kappa$. The $|q,0\rangle_\kappa$ state is less entangled for a larger q such that the just radiated particles become less entangled with the horizon during the radiation process. This result is consistent with the Page curve. For a black hole horizon state, there should be an upper bound on the occupation number N of the horizon states for indicating the mass of the black hole. After radiating N particles, the black hole evaporates. Subsequently, the horizon vacuum sate $|0,0\rangle_\kappa$ should be expended as follows:

$$|0,0\rangle_\alpha = \frac{1}{Z_0}\sum_{n}^{N}\frac{1}{\cosh r}\tanh^n r|n,n\rangle_\kappa \quad (39)$$

Under this upper-bound assumption, We still can continue the radiation process (Eq. (37)) as follows:

$$|0,0\rangle_\kappa \to \frac{1}{Z_m}\sum_{n_m=0}^{N}\sum_{n_{m-1}=0}^{n_m}\cdots\sum_{n_1=0}^{n_2} f_{n_m-n_{m-1}}(n_{m-1},\tanh r_m)\cdots f_{n_1}(0,\tanh r_1)|n_m,0\rangle_{\kappa_m}|n_m-n_{m-1}\rangle\cdots|n_1\rangle \quad (40)$$

We firstly consider Eq. (40) when the surface gravity remains unchanged over time such that $r \equiv r_m = r_{m-1} = \cdots = r_1$. This is a simplified situation that is easy to analytically calculate. The horizon density matrix can be obtained by tracing the radiation part, and in this case, it has a simple form as follows:

$$\frac{1}{Z_m}\sum_{n_m=0}^{N}\sum_{n_{m-1}=0}^{n_m}\cdots\sum_{n_1=0}^{n_2} f^2_{n_m-n_{m-1}}(n_{m-1},\tanh r)\cdots f^2_{n_2-n_1}(n_1,\tanh r)f^2_{n_1}(0,\tanh r)|n_m,0\rangle_\kappa\langle n_m,0| = \frac{1}{Z_m}\sum_{n_m}^{N}\frac{1}{\cosh^{2m} r}\left(1-\frac{1}{\cosh^{2m} r}\right)^{n_m}|n_m,0\rangle_\kappa\langle n_m,0| \quad (41)$$

Therefore, for more radiation steps m, there is a higher probability of obtaining a horizon state $|n_m,0\rangle$, which is larger than n_m. Moreover, after infinite steps, the horizon state is $|N,0\rangle$ with a probability of one.

If the horizon state is observed at a certain time and in a state $|n_m,0\rangle$, then radiation is now in a pure state:

$$\frac{1}{Z}\sum_{n_{m-1}=0}^{n_m}\cdots\sum_{n_1=0}^{n_2} f_{n_m-n_{m-1}}(n_{m-1},\tanh r)\cdots f_{n_2-n_1}(n_1,\tanh r)f_{n_1}(0,\tanh r)|n_m,0\rangle_{\kappa_m}|n_m-n_{m-1}\rangle\cdots|n_1\rangle \quad (42)$$

The density matrix of the just radiated particles can be obtained by tracing the early radiation as follows:

$$\frac{1}{Z}\sum_{n_{m-1}=0}^{n_m}\cdots\sum_{n_1=0}^{n_2} f^2_{n_m-n_{m-1}}(n_{m-1},\tanh r)\cdots f^2_{n_2-n_1}(n_1,\tanh r)f^2_{n_1}(0,\tanh r)|n_m,0\rangle_{\kappa_m}|n_m-n_{m-1}\rangle\langle n_m-n_{m-1}| = \sum_{n_{m-1}=0}^{n_m}\frac{m_n!}{(n_m-n_{m-1})!n_{m-1}!}\frac{(1-\tanh^2 r)^{n_{m-1}}\left(1-(1-\tanh^2 r)^{m-1}\right)^{n_{m-1}}}{\left(1-(1-\tanh^2 r)^m\right)^{n_m}}\cdot \tanh^{2(n_m-n_{m-1})} r|n_m-n_{m-1}\rangle\langle n_m-n_{m-1}| \quad (43)$$

In particular, when $m \to \infty$, the density matrix of just radiated particles is as follows:

$$\sum_{n_{m-1}=0}^{n_m}\frac{m_n!}{(n_m-n_{m-1})!n_{m-1}!}(1-\tanh^2 r)^{n_{m-1}}\cdot (\tanh r)^{2n_m-2n_{m-1}}|n_m-n_{m-1}\rangle\langle n_m-n_{m-1}| \quad (44)$$

Now, we can calculate the von Neumann entropy of this matrix, which has the same entropy as early radiation. For

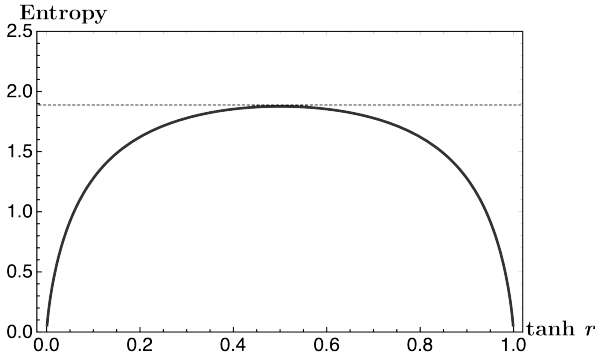

Fig. 6. Entropy of the radiation after m steps when considering the simplification situation that assumes fixed surface gravity and $m \to \infty$. The vertical axis corresponds to the von Neumann entropy of radiation, and the horizontal axis is $\tanh r_{m-1}$. This quantifies the surface gravity of the last radiating process. The results show that the radiation entropy increases from zero at zero surface gravity and decreases to zero at infinitely large surface gravity.

DOI: 10.52396/JUSTC-2022-0039
JUSTC, **2022**, 52(6): 4

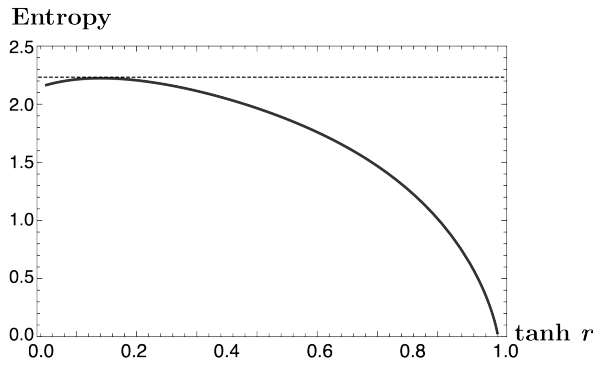

Fig. 7. Entropy of the radiation after m steps when considering surface gravity changes during the radiation process. In this case, we manually select certain values of r_i. The vertical axis is the von Neumann entropy of radiation, and the horizontal axis is $\tanh r_{m-1}$, which quantifies the surface gravity of the last radiating process. The results show that the radiation entropy increases from zero at zero surface gravity and decreases to zero at infinitely large surface gravity.

this simplified situation, The change in entropy with respect to surface gravity is shown in Fig. 6.

For the varied values of surface gravity situation in Eq. (40), after setting the values of $\{r_m\}$, we can perform the similar calculation to obtain the entropy of early radiation. We manually select $\{r_i\}$ values for each step except r_{m-1}, and the entropy evaluated with $\tanh r_{m-1}$ is shown in Fig. 7.

Both Fig. 6 and Fig. 7 show that as surface gravity increases, the entropy of early radiation will decrease at a later time, and the radiation entropy will be zero as surface gravity becomes infinitely large. As the same before, the black hole will finally evaporate and be in state $|N,0\rangle$ with a probability of one, and the radiation in our model will finally be in a pure state and exhibit zero entropy.

5 Conclusions

In this study, we discussed the energy and entropy properties of the $|q,0\rangle_\alpha$ and $|0,q\rangle_\alpha$ states in the accelerating reference frame. Furthermore, based on the result, we constructed a model of black hole radiation, which led to the "memory effect" in the black hole horizon.

In the accelerating reference frame, the fields exhibit the Unruh effect. We determined that state $|q,0\rangle_\alpha$ right wedge maintains the vacuum thermal property in the inertial reference frame and accelerating reference frame. However, they behave differently in terms of entanglement. We proposed a black-hole radiation model with a horizon described by states $\{|q,0\rangle_\kappa\}$. After the particles fall in a black hole, the black hole horizon vacuum shifts to another state in this set, where q indicates the number of infalling particles. These new horizon states will exhibit a higher probability of emitting more excited particles, and radiated particles will become less entangled with the black hole.

Moreover, after imposing a cutoff on occupation number to indicate the size of the black hole Hilbert space, our model reproduced the Page curve. This implies that the radiation is in a pure state after the black hole completely evaporates. This result preserves the quantum unitarity in the black hole radiation process, and the black hole information paradox does not occur.

We discuss the possibility that the black hole horizon is not a trivial vacuum but has a structure. The horizon still exhibits no hair locally, and when performing a local measurement, such as counting particle numbers, the different horizon states are indistinguishable. However, this entanglement structure has a global effect and can impose the black-hole information in the quantum state of radiation.

Acknowledgements

This work was supported by the National Key R&D Program of China (2021YFC2203100), the National Natural Science Foundation of China (11961131007, 11653002), the Fundamental Research Funds for the Central Universities (WK2030000044), the CSC Innovation Talent Funds, the CAS Project for Young Scientists in Basic Research (YSBR-006), the USTC Fellowship for International Cooperation, and the USTC Research Funds of the Double First-Class Initiative.

Conflict of interest

The author declares that he has no conflict of interest.

Biographies

Jianyu Wang is a postgraduate student of Department of Astronomy, University of Science and Technology of China. His research interests include black holes and Hawking radiation.

References

[1] Fulling S A. Nonuniqueness of canonical field quantization in Riemannian space-time. *Physical Review D,* **1973**, *7* (10): 2850–2862.
[2] Unruh W G, Wald R M. Acceleration radiation and the generalized second law of thermodynamics. *Physical Review D,* **1982**, *25* (4): 942–958.
[3] Unruh W G, Wald R M. What happens when an accelerating observer detects a Rindler particle. *Physical Review D,* **1984**, *29* (6): 1047–1056.
[4] Unruh W G. Thermal bath and decoherence of Rindler spacetimes. *Physical Review D,* **1992**, *46* (8): 3271–3277.
[5] Unruh W G. Acceleration radiation for orbiting electrons. *Physics Reports,* **1998**, *307*: 163–171.
[6] Crispino L C, Higuchi A, Matsas G E. The Unruh effect and its applications. *Reviews of Modern Physics,* **2008**, *80* (3): 787–838.
[7] Bekenstein J D. Generalized second law of thermodynamics in black-hole physics. *Physical Review D,* **1974**, *9* (12): 3292–3300.
[8] Unruh W G. Second quantization in the Kerr metric. *Physical Review D,* **1974**, *10* (10): 3194–3205.
[9] Hawking S W. Particle creation by black holes. *Communications in Mathematical Physics,* **1975**, *43* (3): 199–220.
[10] Unruh W G. Notes on black-hole evaporation. *Physical Review D,* **1976**, *14* (4): 870–892.
[11] Dabholkar A, Nampuri S. Quantum black holes. In: Baumgartl M, Brunner I, Haack M, editors. Strings and Fundamental Physics. Berlin: Springer, 2012: 165–232.
[12] Lambert P H. Introduction to black hole evaporation. *Proceedings of Science,* **2014**: PoS(Modave 2013)001.
[13] Socolovsky M. Rindler space, Unruh effect and Hawking temperature. *Annales de la Fondation Louis de Broglie,* **2014**, *39*: 1–49.

DOI: 10.52396/JUSTC-2022-0039
JUSTC, **2022**, 52(6): 4

[14] Alsing P M, Fuentes-Schuller I, Mann R B, et al. Entanglement of Dirac fields in noninertial frames. *Physical Review A,* **2006**, *74* (3): 032326.
[15] Martín-Martínez E, León J. Quantum correlations through event horizons: Fermionic versus bosonic entanglement. *Physical Review A,* **2010**, *81* (3): 032320.
[16] Martín-Martínez E, Fuentes I. Redistribution of particle and antiparticle entanglement in noninertial frames. *Physical Review A,* **2011**, *83* (5): 052306.
[17] Wang J, Jing J. Multipartite entanglement of fermionic systems in noninertial frames. *Physical Review A,* **2011**, *83* (2): 022314.
[18] Wipf A. Quantum fields near black holes. In: Hehl F W, Kiefer C, Metzler R J K, editors. Black Holes: Theory and Observation. Berlin: Springer, 2003: 385–415.
[19] Susskind L, Lindesay J. An Introduction to Black Holes, Information and the String Theory Revolution: The Holographic Universe. Singapore: World Scientific Publishing Co. Pte. Ltd., 2004.
[20] Fuentes-Schuller I, Mann R B. Alice falls into a black hole: Entanglement in noninertial frames. *Physical Review Letters,* **2005**, *95* (12): 120404.
[21] Jacobson T. Introduction to quantum fields in curved spacetime and the Hawking effect. In: Gomberoff A, Marolf D, editors. Lectures on Quantum Gravity. Boston, MA: Springer, 2005: 39–89.
[22] Semay C. Penrose-Carter diagram for a uniformly accelerated observer. *European Journal of Physics,* **2007**, *28* (5): 877–887.
[23] Alsing P M, Fuentes I. Observer-dependent entanglement. *Classical and Quantum Gravity,* **2012**, *29* (22): 224001.
[24] Higuchi A, Iso S, Ueda K, et al. Entanglement of the vacuum between left, right, future, and past: The origin of entanglement-induced quantum radiation. *Physical Review D,* **2017**, *96* (8): 083531.
[25] Bruschi D E, Louko J, Martín-Martínez E, et al. Unruh effect in quantum information beyond the single-mode approximation. *Physical Review A,* **2010**, *82* (4): 042332.
[26] Adesso G, Fuentes-Schuller I, Ericsson M. Continuous-variable entanglement sharing in noninertial frames. *Physical Review A,* **2007**, *76* (6): 062112.
[27] Alsing P M, Milburn G J. Teleportation with a uniformly accelerated partner. *Physical Review Letters,* **2003**, *91* (18): 180404.
[28] Dai Y, Shen Z, Shi Y. Killing quantum entanglement by acceleration or a black hole. *Journal of High Energy Physics,* **2015**, *2015*: 71.
[29] Datta A. Quantum discord between relatively accelerated observers. *Physical Review A,* **2009**, *80* (5): 052304.
[30] Santana A E, Malbouisson J M C, Malbouisson A P C, et al. Thermal field theory: Algebraic aspects and applications to confined systems. In: Khanna F, Matrasulov D, editors. Non-Linear Dynamics and Fundamental Interactions. Dordrecht, Netherlands: Springer, 2006: 187–213.
[31] Mukohyama S. Hartle-Hawking state is a maximum of entanglement entropy. *Phys. Rev. D,* **2000**, *61*: 064015.
[32] Jacobson T. Black holes and Hawking radiation in spacetime and its analogues. In: Faccio D, Francesco B, Cacciatori S, et al, editors. Analogue Gravity Phenomenology. Cham, Switzerland: Springer, **2013**: 1–29.
[33] Martín-Martínez E, Garay L J, León J. Unveiling quantum entanglement degradation near a Schwarzschild black hole. *Physical Review D,* **2010**, *82* (6): 064006.
[34] Venkataratnam K K. Analytical study of two-mode thermal squeezed states and black holes. *International Journal of Theoretical Physics,* **2017**, *56* (2): 377–385.
[35] Dhayal R, Rathore M, Venkataratnam K K. Single-mode squeezed thermal states and black holes. *International Journal of Theoretical Physics,* **2019**, *58* (12): 4311–4322.
[36] Hawking S W. Breakdown of predictability in gravitational collapse. *Physical Review D,* **1976**, *14* (10): 2460–2473.
[37] Mathur S D. The information paradox: A pedagogical introduction. *Classical and Quantum Gravity,* **2009**, *26* (22): 224001.
[38] Unruh W G, Wald R M. Information loss. *Reports on Progress in Physics,* **2017**, *80* (9): 092002.
[39] Page D N. Average entropy of a subsystem. *Physical Review Letters,* **1993**, *71* (9): 1291–1294.
[40] Page D N. Information in black hole radiation. *Physical Review Letters,* **1993**, *71* (23): 3743–3746.

DOI: 10.52396/JUSTC-2022-0039
JUSTC, **2022**, 52(6): 4